Soft Matter

RSC Publishing

PAPER

View Article Online
View Journal | View Issue



Cite this: *Soft Matter*, 2013, **9**, 1817

# A comparison of short-range molecular order in bent-core and rod-like nematic liquid crystals

S. Chakraborty,[a] J. T. Gleeson,[a] A. Jakli[bc] and S. Sprunt*[a]

Received 20th September 2012
Accepted 13th November 2012

DOI: 10.1039/c2sm27177j

www.rsc.org/softmatter

Thermotropic liquid crystals exhibit strongly temperature-dependent positional correlations among molecules in the nematic phase above the transition to a smectic-A or C phase. However, even in the absence of a lower temperature smectic phase, nematics composed of reduced symmetry molecules (bent-core mesogens, for example) reveal small angle X-ray scattering (SAXS) patterns with features similar to those associated with pretransitional smectic order. We report on a quantitative analysis and comparison of two-dimensional SAXS data on a bent-core nematic compound (lacking a smectic phase) and a rod-like nematic (exhibiting a nematic to smectic-C transition). This analysis demonstrates that a nanostructure based on distinct, smectic-C ordered molecular clusters provides a more accurate account of the diffraction data from the bent-core nematic than the standard models used to describe fluctuating smectic order in rod-like nematics. The average dimensions of the clusters are weakly temperature dependent, while the interlayer spacing and layer tilt angle with respect to the average molecular long axis are temperature independent. Our results may help to explain interesting and unusual macroscopic properties recently discovered in the fluid phases of bent-core molecules.

## I Introduction

The nature of short-range intermolecular order in bent-core nematic liquid crystals, and the interpretation of small angle X-ray scattering (SAXS) measurements probing this order, are issues that have generated both significant interest and debate within the liquid crystals' community over recent years. On the one hand, the observation of four-lobe patterns in the SAXS intensity for aligned bent-core nematics has been construed[1–4] as evidence of short-range tilted (smectic-C-like) layer correlations similar to the pretransitional smectic-C order or so-called "cybotactic groups"[5] observed in ordinary calamitic (rodlike) nematics. Alternatively, the SAXS pattern has been considered[6] to be a signature of biaxial orientational order, with the four small angle peaks arising from the molecular form factor in the situation where the long (end to end) and short (transverse) molecular axes of the bent-shaped molecules align spontaneously along orthogonal directions in space. This scenario differs fundamentally from the "cybotactic groups" because the biaxial order is assumed to be long range – *i.e.*, of order the X-ray beam size – and purely orientational in nature, rather than contained within short-range positionally-correlated molecular arrangements.

The present paper concerns bent-core nematics that show no evidence of macroscopic biaxiality. Its aim is to demonstrate a distinct difference between two types of short-range order in nematics: pretransitional smectic order, demonstrated in common calamitic nematics, and a discrete, smectic-like clustering of molecules that we argue characterizes the local organization in nematics formed from certain bent-core and potentially other types of reduced symmetry mesogens. We perform the comparison through a quantitative analysis of SAXS intensity contours recorded on a rodlike compound (that exhibits a nematic–smectic-C transition) and a bent-core material (that lacks one). The structure and phase sequence of the two molecules are shown in Fig. 1(a); we refer to the rodlike molecule, 4-*n*-octyloxyphenyl 4′-*n*-hexyloxy-benzoate,[7] as 6OO8, and to the bent-core compound, 4,6-dicholoro-1,3-phenylene bis-4-[4′-(dodecyloxy))biphenyl] carboxylate,[8] as DClPbis12BC. Optical conoscopy and light scattering experiments clearly indicate that the nematic mesophase of the DClPbis12BC is uniaxial.

Our main results are the following: above the smectic-C transition in the calamitic liquid crystal, the SAXS contours are correctly described in the framework of a Landau–de Gennes theory, which leads to a Lorentzian lineshape[9] that must be modified at lower temperatures due to the strong coupling of smectic layer fluctuations to the nematic director.[10,11] This lineshape has been successfully applied to calamitic nematics in classic, high-resolution X-ray studies,[12–14] and we confirm similar results utilizing 2D SAXS data on the compound 6OO8. However, for the bent-core compound, we find that the modified Lorentzian model for smectic correlations fails to describe

[a]*Department of Physics, Kent State University, Kent, OH, 44242 USA. E-mail: ssprunt@kent.edu*

[b]*Liquid Crystal Institute, Kent State University, Kent, OH 44242, USA*

[c]*Chemical Physics Interdisciplinary Program, Kent State University, Kent, OH 44242, USA*

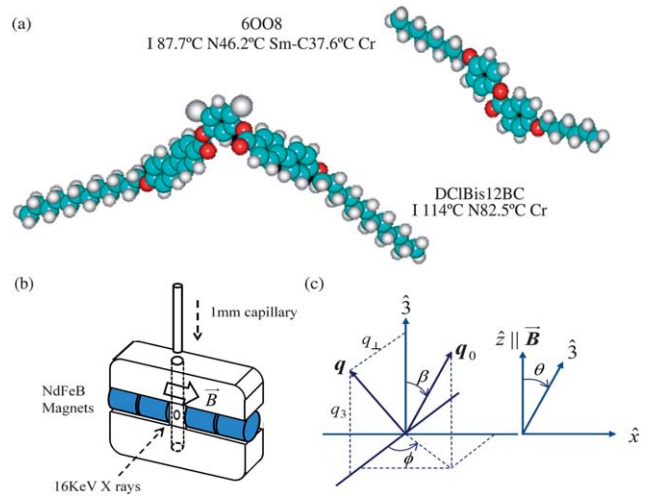


**Fig. 1** (a) Chemical structure and phase sequences of the LC compounds studied. (b) Sample cassette used in the SAXS measurements. (c) At left: the scattering vector $\vec{q}$ and the layering wavevector $\vec{q}_0$ in the local frame of a smectic correlated volume; the unit vector $\hat{3}$ designates the average molecular long axis, and $\beta$ is the layer tilt angle with respect to this axis. At right: polar angle $\theta$ describing a distribution of the $\hat{3}$ direction in the laboratory frame; $\vec{B}$ is the magnetic field applied to align the nematic director, and $x$–$z$ plane is the plane of the detector.

accurately the SAXS contours over the nematic range. Instead, we demonstrate that a lineshape based on distinct, internally ordered smectic-C-like molecular clusters, described by three anisotropic, weakly temperature-dependent lengths of order 1–10 nm, produces a better quantitative account of the full set of 2D diffraction data. The only significantly temperature-dependent quantity is the width of the angular distribution that characterizes the orientation of the clusters; this width increases below the nematic–isotropic transition in accordance with the behavior expected for the nematic order parameter. The smectic "cluster" model has been proposed before as an explanation for interesting and unusual macroscopic properties of bent-core nematics, including unusual anisotropy in orientational elastic moduli and viscosities,[15,16] large flexoelectricity,[17] and non-Newtonian flow rheology,[18] but there has been no decisive test of this model, based on a widely applicable structural technique such as SAXS, in materials that specifically exhibit these properties. Our results fulfill this need.

## II Experimental details

For our studies, samples of DClPbis12BC and 6OO8 were loaded in powder form into untreated, cylindrical fused quartz capillaries with 1 mm inner diameter and 0.01 mm wall thickness. The samples were then melted into the isotropic fluid phase and repeatedly shaken in order to release any trapped air bubbles and to ensure complete filling of the bottom 4 mm of the capillary. The filled capillary was inserted into an aluminum cassette [Fig. 1(b)], which has a central 1.5 mm hole to admit the X-ray beam and allow collection of small-angle forward scattering from the sample. Positioned on opposite sides of the capillary are 12.7 mm diameter × 25.4 mm long, cylindrical neodymium iron boron magnets (high temperature grade N42SH), which were used for magnetic alignment of the average molecular long axis of the nematic (uniaxial director $\vec{n}$). The pole separation is 2.5 mm, and the field in the middle of the gap (across the sample) was measured to be 1.2 T.[19]

The sample cassette was placed inside a commercial hot stage (Instec, model HCS402) that allowed the sample temperature to be controlled within ±0.05 °C. The hot stage was then mounted inside a vacuum chamber, which is secured to the X-ray flight path on beam line X6B at the National Synchrotron Light Source (NSLS, Brookhaven National Laboratory) and evacuated to eliminate background scattering from air. The incident X-ray energy was 16.0 keV (wavelength $\lambda = 0.775$ Å), and the spot size was slitted down to a cross-section of approximately 0.2 × 0.3 mm at the sample. We aligned the nematic director by heating the samples to the isotropic phase and then slowly cooling them into the nematic state in the presence of the applied magnetic field (which is normal to the incident beam direction). SAXS patterns were recorded at fixed temperature intervals in cooling on a 2084 × 2084 pixel area detector, located 1.2 m from the samples and approximately centered on the incident beam. The typical acquisition time was 240 s. We calibrated the pixel position on the detector against scattering wavenumber using silver behenate powder that was filled into a capillary identical to those used for the LC samples. In addition, the pattern of scattering from an empty capillary was recorded; this showed no systematic features different from an image taken without any capillary present. The experimental resolution in scattering wavenumber is approximately 0.0033 $\text{Å}^{-1}$.

The recorded diffraction images were processed using the commercial software package DataSqueeze to produce exportable data files, as described in ref. 1. From these, we extracted sets of 2D contours and 1D cuts in $q$-space with the software package IGOR, and performed subsequent analysis using the nonlinear least squares fitting routines in Mathematica.

## III Theoretical background

The intensity of X-ray scattering from short-range smectic order in a nematic LC is proportional to scattering structure factor $S(\vec{q})$, which is given by the Fourier transform of the density correlation function. To calculate $S(\vec{q})$ arising from smectic correlations in a nematic phase, the conventional approach is to start with a Landau–de Gennes expansion of the free energy in the relevant order parameters – *e.g.*, the complex order parameter $\psi$ describing the smectic density wave, the nematic director $\vec{n}$, and a separate tilt order parameter (usually taken as a two component vector $\vec{c}$ representing the projection of $\vec{n}$ into the smectic layer plane) to account for "skewed" stacking of layers relative to $\vec{n}$ (smectic-C-type layering). One then calculates the mean square Fourier amplitude $\left\langle |\psi(\vec{q})|^2 \right\rangle$, including terms in the free energy up to quadratic order in the fluctuating quantities. Finally, higher order couplings of $\psi,\vec{n},\vec{c}$ may be treated perturbatively, leading to corrections to $\left\langle |\psi(\vec{q})|^2 \right\rangle$. The models analyzed by Chu–McMillan[9] and Andereck–Patton (AP)[11] incorporate the tilt order parameter explicitly, and lead to a Lorentzian form for $S(\vec{q})$, with peaks centered on wavevectors $\pm\vec{q}_0$ corresponding to a density wave tilted with respect to $\vec{n}$. In

 

the vicinity of the transition to a smectic-C phase ($T_{NC}$), the AP calculation includes the effect of higher order couplings in the free energy, and predicts corrections of order $q^4$ to a Lorentzian lineshape. Similar behavior is obtained from a theory, due to Chen and Lubensky,[10] where the tilt enters through gradients in $\psi$ without invoking a separate tilt order parameter.

The resulting "modified" Lorentzian form for $S(\vec{q})$ is expressed in terms of $\vec{q}_0$, two temperature dependent correlation lengths $\xi_\perp$, $\xi_\parallel$ describing fluctuations of smectic order in a uniaxial nematic, and two temperature dependent coefficients (that we denote $c_2$, $c_4$)determining the relative weight of $q^2$ and $q^4$ contributions to the lineshape. If we define $\vec{q}_0$ and the scattering vector $\vec{q}$ in the local frame of a correlated smectic volume, where $\hat{3}$ labels the average long molecular axis, $\perp$ labels the plane perpendicular to this axis, $\beta$ is the layer tilt angle, and $\phi$ is the azimuthal angle defining the orientation of $\vec{q}_0$ in the $\perp$ plane [as shown in Fig. 1(c)], the structure factor obtained by AP may be written:

$$S(q_\perp, q_3) = \sum_{+,-} \int_0^{2\pi} d\phi \frac{S_0}{1 + \xi_\parallel{}^2(q_3 \pm q_{03})^2 + \sum_{n=1,2} c_{2n}\xi_\perp{}^{2n}\left(q_\perp{}^2 + q_{03}{}^2\tan^2\beta - 2q_\perp q_{03}\tan\beta\cos\phi\right)^n} \quad (1)$$

Here $q_{03}$ is the component of $\vec{q}_0$ along $\hat{3}$. Note that the expression in parentheses containing the $q_\perp$ dependence is just the expanded version of $(\vec{q}_\perp - \vec{q}_{0\perp})^2$, where $\vec{q}_\perp \cdot \vec{q}_{0\perp} = q_\perp q_{0\perp}\cos\phi$ and $q_{0\perp} = q_{03}\tan\beta$.

The symbol $\sum_{+,-}$ in eqn (1) implies the sum of separate integrands containing $q_3 + q_{03}$ and $q_3 - q_{03}$, while the integral over $\phi$ accounts for the fact that in the typical experimental situation, the direction $\hat{3}$ is aligned by an external field, and the orientation of $\vec{q}_0$ (*i.e.*, the layer normal) is azimuthally degenerate around $\hat{3}$ [Fig. 1(c)]. This integral can be done analytically,[11] but the expression is complicated and we will not reproduce it here. As noted above, the term with coefficient $c_2$ ($n = 1$) in the denominator corresponds to the standard Lorentzian lineshape (obtained from the Landau–de Gennes expansion up to quadratic order), while the $c_4$ term ($n = 2$) represents the correction due to higher than quadratic order couplings of $\psi,\vec{n},\vec{c}$ in the free energy. The coefficients $c_2$ and $c_4$ are non-negative and temperature-dependent, with $c_2 \to 1$ and $c_4 \to 0$ far from a nematic to smectic-C transition. [The reason that no correction of order $(q_3 \pm q_{03})^4$ is included is that the quadratic terms $(q_3 \pm q_{03})^2$ always dominate, even close to the NC transition; however, this is *not* the case for the $q_\perp$ contributions.[11]] When $c_4 = 0$, the $\phi$ integral yields a product of square roots of Lorentzians,[9] which is symmetric under $q_\perp \to -q_\perp$.

At finite temperature the local orientation of correlated volumes ($\hat{3}$) fluctuates with respect to the direction of the aligning field $\vec{B}$, and so the $\hat{3}$ direction is subject to a statistical distribution in the lab frame. For simplicity, in Fig. 1(c) we show only the polar angle $\theta$ specifying the orientation of $\hat{3}$ relative to $\vec{B}$ in the $x$–$z$ plane of the detector. In addition to thermal fluctuations, there will be a mosaicity due to defects and variations in the axis of nematic alignment, which could occur near the curved surfaces of the cylindrical capillary. For temperatures approaching the nematic to isotropic transition ($T_{NI}$), the inverse width of the orientational distribution (denoted by a parameter $\gamma$) should scale with the nematic order parameter (through the diamagnetic susceptibility anisotropy that couples to $\vec{B}$). Then using the Maier–Saupe form for the distribution of $\hat{3}$, and designating $\vec{Q}$ as the scattering vector in the lab coordinates ($x$, $y$, $z$ with $x$–$z$ being the detector plane), we may write the following expression for $S(\vec{Q})$,

$$S(\vec{Q}) = \int d\Omega\, \exp(-\gamma\sin^2\theta) S[q_\perp(\Omega;\, \vec{Q}), q_3(\Omega;\, \vec{Q})] \quad (2)$$

When the scattering angle $\alpha$ is small (as in the SAXS experiment), the major components of $\vec{Q}$ are $Q_x$, $Q_z \sim \alpha$ while $Q_y \sim \alpha^2$ is negligible. Thus, it is a reasonable approximation to consider only the $Q_x$, $Q_z$ dependence of $q_\perp$ and $q_3$.

For a nematic that does not exhibit a lower temperature transition to a smectic-A or C phase, but nevertheless shows evidence in the SAXS pattern for short-range layer structure, one may also consider a Lorentzian form for $S(\vec{q})$, because this form may always be obtained from a general Ornstein–Zernike expansion of molecular density correlations. However, the unusual macroscopic properties of bent-core nematics noted in the Introduction, the propensity of bent-shaped molecules to pack in layers to conserve space, and the comparative rarity of nematic phases observed in bent-core LCs, point to another possibility – namely, finite size, smectic-ordered molecular clusters that are quasi-equilibrium structures, rather than fluctuating, pretransitional entities. This scenario was originally proposed ten years ago,[20] and a theoretical framework to describe a nematic fluid formed from such clusters was later presented.[21]

We can develop a fairly simple expression for scattering from smectic-ordered nanoclusters as follows. First, if we imagine the clusters as well-defined smectic-C-like domains of finite extent ($L_1 \times L_2 \times L_3$ in the local Cartesian frame of a cluster), the structure factor is proportional to the product $\prod_{i=1-3} \frac{\sin^2[(q_i - q_{0i})L_i/2]}{[(q_i - q_{0i})L_i/2]^2}$. Then, to account for the physically realistic situation where the interfaces between clusters are not perfectly sharp and/or the cluster dimensions are statistically distributed about mean values, the Warren approximation[22] may be applied, leading to a Gaussian lineshape.[23] In this case, the azimuthal average accounting for layer tilt degeneracy with respect to the $\hat{3}$ direction can be done analytically when the $L_1 = L_2$, but must be carried out numerically otherwise. For the finite smectic "cluster" model, the expression for $S(q_z, q_\perp)$ that supersedes eqn (1) is

$$S(q_3, q_\perp) = \sum_{+,-} S_0 \exp\left[-\sigma_3{}^2(q_3 \pm q_{03})^2\right] \times \int_0^{2\pi} d\phi \exp[-\sigma_1{}^2(q_\perp{}^2 + q_{03}{}^2\tan^2\beta - 2q_\perp q_{03}\tan\beta\cos\phi) - \Delta\sigma^2 q_\perp{}^2\sin^2\phi] \quad (3)$$

where $\Delta\sigma^2 = {\sigma_2}^2 - {\sigma_1}^2$, and the Gaussian widths $\sigma_i$ are related to the average cluster dimensions $L_i$ by $L_i = 2\sqrt{\pi}\sigma_i$.[23] The symbol $\sum_{+,-}$ has the same meaning as in eqn (1).

As noted, the integrals in eqn (1) and (3) cannot generally be evaluated analytically, and, where this is possible, yield rather complicated functions of $q_3$, $q_\perp$. Given this fact and in order to make numerical computation of the orientational averages in eqn (2) manageable in our data analysis, we restricted the 3D orientational average to a 2D (plane polar) average. Specifically, we replaced the integral over solid angle with a single integral over the polar angle $\theta$ indicated in Fig. 1(c) and used the relations $q_3 = \sin\theta Q_x + \cos\theta Q_z$, $q_\perp = \cos\theta Q_x - \sin\theta Q_z$ to express the scattering vector $\vec{q}$ in the local frame of the smectic layers in terms of components of $\vec{Q}$ in the plane of the detector. Thus, we substituted for eqn (2) the restricted average,

$$S\left(\vec{Q}\right) = \int_{-\pi/2}^{\pi/2} \mathrm{d}\theta \exp\left(-\gamma\sin^2\theta\right) S\left[q_\perp\left(\theta;\vec{Q}\right), q_3\left(\theta;\vec{Q}\right)\right] \quad (4)$$

In the data analysis described in the next section, we found no significant variation in fit quality or parameter values using the restricted *versus* full orientational averaging.

## IV Results and discussion

### A Calamitic nematic 6OO8

In our analysis of the SAXS data for 6OO8, we focused mainly on the upper nematic range, away from the transition to the smectic-C phase. This choice is more apt for comparison to smectic correlations in a bent-core nematic compound that lacks a bulk smectic phase. The top row of Fig. 2 shows representative SAXS images for three temperatures in the upper half of the nematic ($T_{NI} - T = 2$, 15, and 23 °C) and one temperature ($T_{NI} - T = 41$ °C) close to the nematic to smectic-C transition. The direction of the applied magnetic field is vertical, and the ranges of $Q_z$ and $Q_x$ are displayed on the vertical and horizontal axes, respectively. (The diffraction images are symmetrical about $Q_z = 0$; only the patterns in the half plane $Q_z > 0$ are shown.) With decreasing temperature from $T_{NI}$, the diffraction pattern evolves from a broad peak in $Q_x$ centered on $Q_x = 0$ and $Q_z \simeq 0.2$ Å$^{-1}$ to separate, narrower peaks positioned at finite $\pm Q_x$. Closer to the smectic-C transition, these peaks sharpen in both $Q_x$ and $Q_z$, as expected from the pretransitional increase in the smectic correlation lengths $\xi_\perp$, $\xi_\parallel$, which has been studied in detail in previous works.[12–14]

In the second row in Fig. 2 are contour plots of the SAXS data, color coded for five different levels of the diffracted intensity (above the gray background level). The third row shows contours at the same levels generated from fits of the data to the modified Lorentzian model, eqn (1) and (4). The fits were performed on a large subset of the full 2D data, comprising six cuts along the $Q_z$ direction, at even intervals of 0.05 Å$^{-1}$ between $Q_x = 0$ and 0.30 Å$^{-1}$, plus a single cut along $Q_x$ at the value of $Q_z$ corresponding to the peak intensity. [Each cut is actually the average of a 10 pixel (0.005 Å$^{-1}$) wide strip of data, centered on the value of $Q_x$ or $Q_z$ selected for the cut.] The fits for different temperatures revealed no systematic variation in the layer tilt angle $\beta$ or the layer wavenumber $q_0$; the data were therefore refit with these fixed to $\beta = 35°$ and $q_{03} = 0.204$ Å$^{-1}$ (which corresponds to $2\pi/L$ where $L$ is the calculated length of a 6OO8 molecule). The variable parameters in the simultaneous fitting to the cuts then included the amplitude $S_0$, correlation length $\xi_\parallel$, renormalized correlation length $\xi'_\perp \equiv \sqrt{c_2}\,\xi_\perp$, renormalized coefficient of the correction term to a Lorentzian lineshape in eqn (1), given by $c'_4\xi'^4_\perp \equiv c_4\xi^4_\perp$ or $c'_4 = c_4/{c_2}^2$, the inverse width of the orientational distribution $\gamma$, and a constant background. In the bottom two rows of Fig. 2, we present similar results from fitting the contour data to the Gaussian lineshape [eqn (3) and (4)], with variable parameters $S_0$, $\sigma_1$, $\sigma_3$, $\Delta\sigma^2$, $\gamma$, and a constant background (again with $\beta = 35°$ and $q_{03} = 0.204$ Å$^{-1}$). Fig. 3 displays scattered intensity *vs.* $Q$ for selected cuts through the 2D data, together with results of the fits to the modified

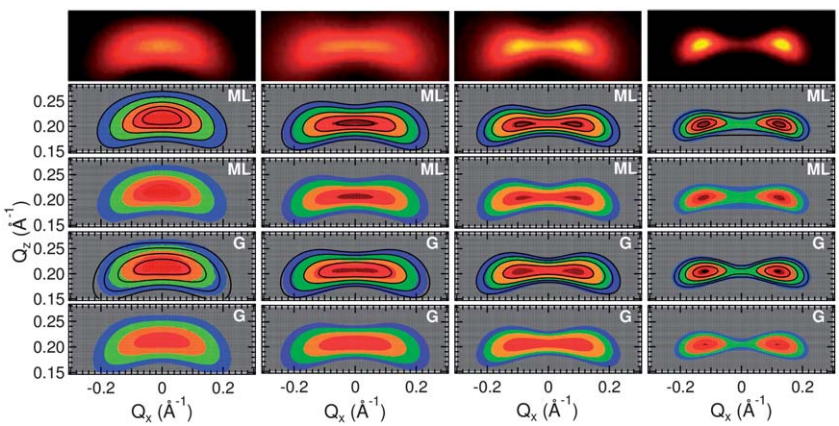


**Fig. 2** Representative results on the calamitic nematic 6OO8. Top row: two dimensional SAXS images recorded at different temperatures $T_{NI} - T = 2$, 15, 23 and 41 °C (left to right, respectively) in the nematic phase. Second row from top: color-coded, constant intensity contours generated from the SAXS data for the same temperatures as in the images immediately above. Black lines at the edges of the color contours are the corresponding intensity levels calculated from fits to the modified Lorentzian (ML) model [eqn (1) and (4)] describing smectic-C correlations in a nematic phase. Third row: false color contours of the fitted ML model at the same intensity levels as the data in the second row. Fourth row: comparison between the data and calculated contours from the best fit (black lines) to the Gaussian (G) lineshape [eqn (3) and (4)]. Fifth row: false color calculated contours from the G model.

 

Lorentzian and Gaussian lineshapes. (The temperatures corresponding to the three columns are the same as the three higher temperatures in Fig. 2.)

The quality of the fits of the data contours and cuts in Fig. 2 and 3 to the modified Lorentzian model is quite good overall, although the fit misses the outermost contours for the lowest temperature ($T_{NI} - T = 41$ °C, 1 °C above the transition to the smectic-C phase). Close to the transition, higher resolution and more careful tuning of $\vec{Q}$ to the Bragg peak is required to accurately determine parameters such as the correlation lengths. For this reason, we do not further consider the low temperature data on 6OO8. The temperature dependence of the parameters $\xi_{\|}$, $\xi'_{\perp}$, $c'_4$, and $\gamma$, extracted from the fitting for the upper nematic range, is shown in Fig. 4. Even far from the smectic-C transition, the correlation lengths increase substantially with decreasing temperature, while the inverse width of the orientational distribution of the correlated volumes decreases on approach to the isotropic phase ($T = T_{NI}$). The renormalized coefficient of the non-Lorentzian term, $c'_4 = {c_4}^2/c_2$, begins to increase (from zero) with decreasing $T$ at $T_{NI} - T \approx 13$ °C. This accords with the theoretical prediction in ref. 11, but it is remarkable that the onset of the increase occurs rather far (~28 °C) above the smectic-C phase. At lower temperature, we find that the value of $c'_4$ levels off. This is also expected from detailed calculations of $c_4$ and $c_2$, but in this temperature range, the fit to the outer contours of the SAXS data starts to break down, likely indicating limitations of the SAXS technique when the smectic layer peaks sharpen dramatically.

Compared to the modified Lorentzian, the fits of the data for 6OO8 to the Gaussian lineshape (with the same number of fit parameters) are of poorer quality, especially in the vicinity of the peak scattered intensity. Specifically, the missing (central) fit contours in the bottom two rows of Fig. 2 reflect the fact that the fit falls significantly below the data in the peak region. Of course the Gaussian model, which describes finite-sized molecular clusters with non-zero internal smectic order, is not expected to apply in the case of fluctuating order above a nematic to smectic transition (as occurs in 6OO8).

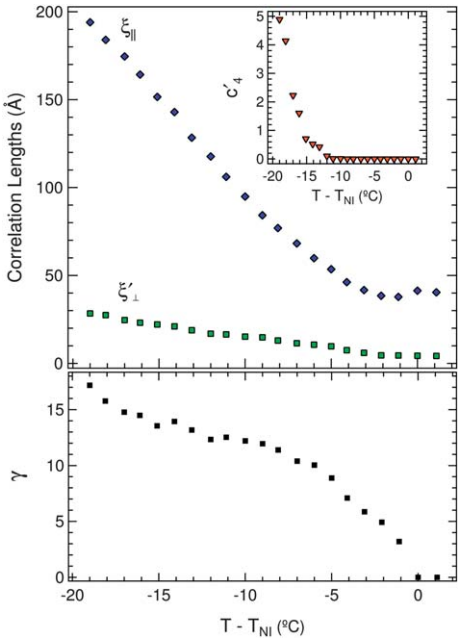


**Fig. 4** Temperature dependence of the smectic correlation lengths, inverse width $\gamma$ of the orientational distribution function, and renormalized coefficient $c'_4$ of the $q^4$ term in the modified Lorentzian lineshape, obtained from fitting the SAXS data for 6OO8 to eqn (1) and (4) in the upper range of the nematic phase.

The model lineshapes used in the analysis in Fig. 2 and 3 assume that the electron density is described by a simple density wave with a period of ~1 molecular length and limited spatial coherence. In particular, we assume that the "lumpiness" within a single molecule does not contribute significantly to the small angle scattering. This is justified because variations in the density that are significantly shorter than the molecular

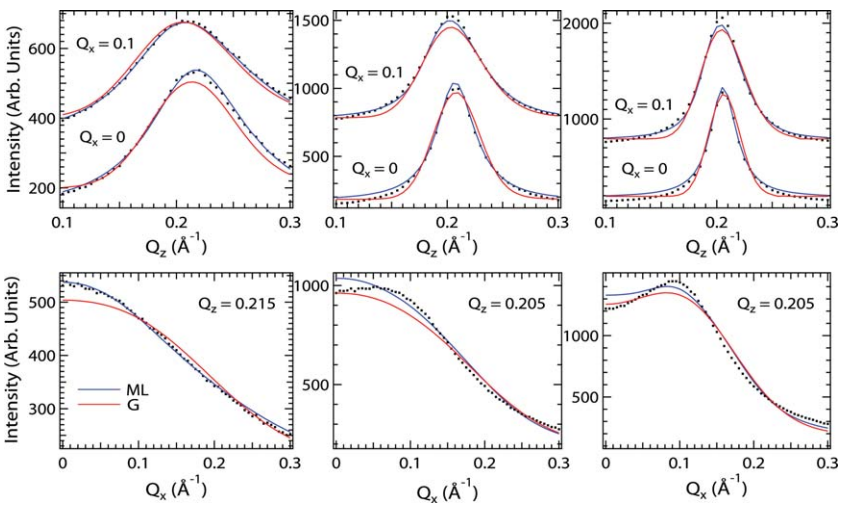


**Fig. 3** Data and fits to the modified Lorentzian (ML) model [eqn (1) and (4)] (blue lines) and to the Gaussian (G) lineshape [eqn (3) and (4))] (red lines) for cuts through the 2D SAXS data on 6OO8. The cuts are taken at the $Q_x$ and $Q_z$ values [Å$^{-1}$] shown in the figure and for temperatures $T_{NI} - T = 2$, 15 and 23 °C (left to right columns, respectively).

length produce variations in scattered intensity (at small angles) that are small over the range of $Q$ corresponding to the width of the observed peaks. Moreover, the quality of the fits in Fig. 2 and 3 (specifically to the modified Lorentzian) does not clearly justify additional fitting parameters.

### B Bent-core nematic DClPbis12BC

We now turn to results for DClPbis12BC. The top two rows of Fig. 5 display SAXS images and contour plots of diffraction data in the same format as Fig. 2 and at representative temperatures $T_{NI} - T = 1$, 12, 29 °C. Qualitatively, the diffraction patterns resemble those shown in Fig. 2 for 6OO8; namely, the single broad peak at $Q_x = 0$ and finite $Q_z$ observed just below the isotropic–nematic transition evolves into two peaks centered on non-zero $\pm Q_x$ at lower temperatures. However, a quantitative analysis using the modified Lorentzian structure factor [eqn (1) and (4)] fails to describe the patterns accurately in the case of the bent-core compound, particularly in the vicinity of the scattering peaks and at low temperature where the peaks split. This failure is demonstrated in the bottom rows of Fig. 5, which show the best fit contours generated from eqn (1) and (4), and in Fig. 6, which plots the fit against various cuts through the data at constant $Q_x$ and $Q_z$. We find (more significantly at lower temperatures) that the modified Lorentzian function cannot simultaneously match the data around the peak intensity and the fairly gradual decay in intensity with large $Q_x$ (relative to the peak value) that occurs in the case of the bent-core material.

On the other hand, the Gaussian model in eqn (3) and (4) based on finite-sized smectic-C-ordered clusters of bent-core molecules, with the same tilt direction between layers (synclinic tilt), provides a good description of the data on DClPbis12BC for all temperatures. The second and third rows in Fig. 5 show a comparison of the fitted contours to the data based on this model, while Fig. 6 shows the fit through 1D cuts for fixed $Q_x$ or $Q_z$ at each temperature. Clearly these fits better represent the full data sets than the modified Lorentzian lineshape. In particular, the term with coefficient $\Delta\sigma^2$ in eqn (3) has the effect of broadening the distribution of intensity at larger $Q_x$, without significantly changing the shape of the contours around the peak intensity. As in the case of the calamitic nematic 6OO8, the analysis reveals that the layer tilt angle and wavenumber are essentially independent of temperature; for DClPbis12BC, these were fixed to the average values of $\beta = 45°$ and $q_{03} = 0.143$ Å$^{-1}$ in order to more precisely determine the parameters $\sigma_1$, $\sigma_3$, $\Delta\sigma^2$, and $\gamma$ in eqn (3) and (4), which were varied in the fitting. The large tilt is typical of the smectic-C phases in bent-core liquid crystals, and the value of $q_{03}$ corresponds to the calculated length of the long axis of a DClPbis12BC molecule.

The temperature dependencies of the average cluster dimensions $L_i$, together with the inverse orientational distribution width parameter $\gamma$, obtained from fits to eqn (3) and (4), are presented in Fig. 7. Recall that $L_3$ corresponds to the direction of the molecular long axis within a cluster, and $L_1$, $L_2$ to two inequivalent orthogonal directions in the plane perpendicular to this axis. In contrast to the lengths $\xi_\perp$ and $\xi_\parallel$ characterizing the smectic correlations in 6OO8, the cluster dimensions in DClPbis12BC vary only weakly with temperature through the nematic range, with $L_1$ and $L_2$ being approximately constant. The parameter $\gamma$ decreases on approach to $T_{NI}$ in the same fashion expected for the nematic order parameter. The anisotropy between $L_1$ and $L_2$ is significant and consistent with the situation that the clusters are quasi-equilibrium entities with lower internal symmetry – *e.g.*, the $D_2$ or $C_2$ symmetry of a

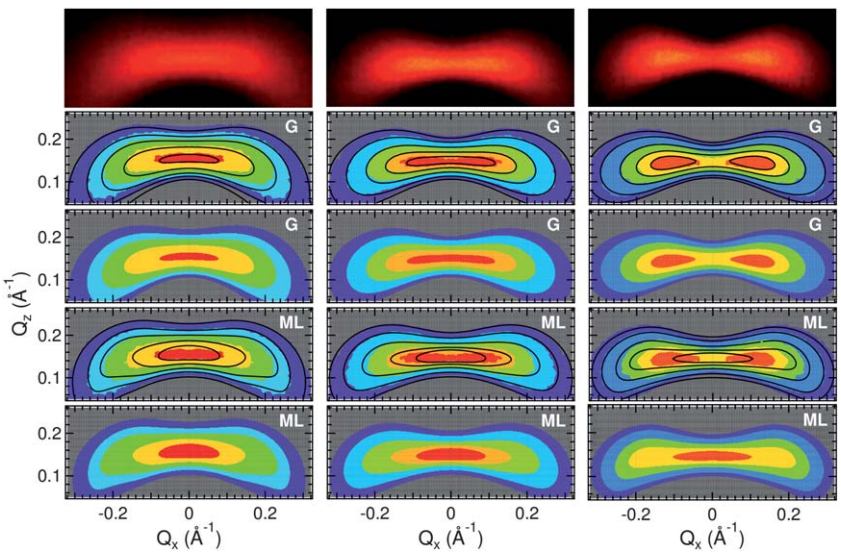


**Fig. 5** Representative results on the bent-core nematic DClPbis12BC. Top row: two dimensional SAXS images recorded at different temperatures $T_{NI} - T = 1$, 12, and 29 °C (left to right, respectively) in the nematic phase. Second row: color-coded, constant intensity contours generated from the SAXS data for the same temperatures as in the images immediately above, together with the corresponding contours (black lines) calculated from fits to the Gaussian (G) model in eqn (3) and (4) describing diffraction from finite-sized smectic-C-ordered molecular clusters. Third row: the calculated contours for the G model shown in false color. Fourth row: comparison between the data and the calculated contours from the best fit (black lines) to the modified Lorentzian (ML) lineshape [from eqn (1) and (4)]. Fifth row: the calculated contours for the ML model shown in false color.

 

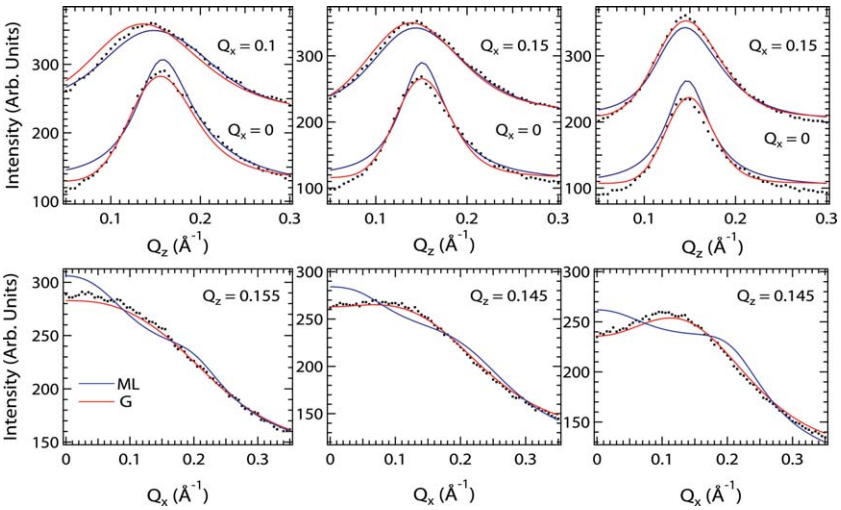


**Fig. 6** Data and fits (red lines) to the Gaussian (G) model in eqn (3) and (4) for various cuts through the 2D SAXS data on DClPbis12BC taken at the constant $Q_x$ or $Q_z$ values [Å$^{-1}$] shown. The temperatures and order of presentation (left to right for decreasing $T$) are the same as in Fig. 5. The blue lines represent best fit to the modified Lorentzian (ML) model [eqn (1) and (4)].

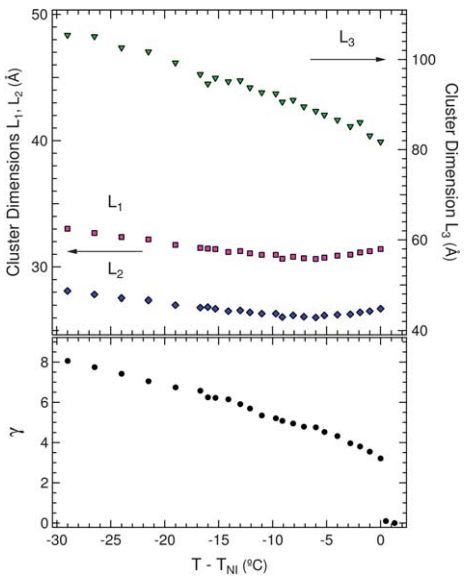


**Fig. 7** Temperature dependence of the average smectic cluster dimensions, $L_i$ ($i$ = 1–3, with the 3 direction corresponding to the average molecular long axis), and inverse width $\gamma$ of the orientational distribution function, obtained from fitting the SAXS data for DClPbis12BC to eqn (3) and (4).

tilted bent-core smectic – than the parent (uniaxial) nematic phase. The typical cluster size is ~3.2 × 2.5 × 9 nm, implying a volume of ~60 molecules and an average of ~2 layers in a cluster.

For completeness, we consider the possibility that the smectic-C-like diffraction pattern with peaks at $(Q_x, Q_z) = (\pm 2\pi\tan\beta/L, \pm 2\pi/L)$ could originate simply from the bent shape of the molecule. Even if we take the optimal scenario for this case – the electron density of a molecule modeled as two uniform rods with sharp edges that connect in a central bend – we would still expect to observe an intense diffuse peak surrounding the main beam at $Q = 0$. This is because the broad peaks associated with the structure factor for short-range intermolecular order do not drop off sufficiently rapidly to cut down the maximum in the molecular form factor at $Q = 0$ when one takes the product of the two contributions. We have performed simple numerical simulations to establish this point. In fact, the actual scattering around $Q = 0$ does not show the simulated diffuse peak (it is no broader than what we observe from an empty capillary). Moreover, while a bent, rigid-rod model for the form factor can in principle generate a four lobe diffraction pattern away from $Q = 0$, the model completely fails to fit the contours of the experimental data around the peaks. On the other hand, as demonstrated, the relatively simple model of a density wave cut off with a Gaussian quantitatively describes the features of the SAXS data on DClPbis12BC rather well. Additionally, we note that mesogens with various shapes (rodlike above a smectic-C phase, bent-core and 'Y'-shaped[24] even in the absence of a smectic phase) produce quite similar smectic-C-like SAXS patterns, whose essential characteristics must therefore be due mainly to the intermolecular organization.

Very recently, smectic-like clusters have been directly imaged in a different bent-core nematic compound by the cryo-TEM technique.[25] The cluster size in that material is apparently more temperature-dependent than our results indicate for DClPbis12BC; the average number of layers per cluster ranges from ~2 to ~4 with decreasing temperature in the nematic range. The lower value (at higher temperature) is consistent with the results in Fig. 7. Currently, the technique is limited to materials where the molecules spontaneously align parallel to a free surface (as opposed to the more common occurrence of perpendicular anchoring).

Finally, we should point out that not all bent-core nematics show short-range smectic-C type order. For example, the addition of side chains to the core of a shape-persistent bent-core compound produces a SAXS pattern indicative of a different type of short-range molecular organization.[26]

## V Conclusion

In this paper, we have used quantitative modeling of 2D small angle X-ray scattering data to demonstrate a fundamental difference between smectic correlations in a conventional calamitic nematic, exhibiting a nematic to smectic-C transition, and a bent-core nematic, which lacks a lower temperature smectic phase but produces similar small angle diffraction. The analysis establishes that the correlations in the bent-core compound are associated with finite-sized, smectic-like molecular clusters, in contrast to the fluctuating, pretransitional smectic order typically observed in calamitics. Our results provide a potentially useful framework to characterize short-range order in nematics formed from other types of reduced-symmetry mesogens – *e.g.*, 'Y'-, 'H'-, or 'W'-shapes. Combined with new resources at advanced SAXS/WAXS synchrotron beamlines (such as NSLS II at Brookhaven National Lab), they may also prove useful in the search for polar or chiral properties on the nanoscale that could spur new technological interest in thermotropic nematics.

## Acknowledgements

We are very grateful to Vesna Stanic and Elaine diMasi for their expert assistance with the set-up and SAXS measurements on beamline X6B at NSLS, and to S. H. Hong and R. Verduzco for their help in the data collection and initial analysis. The liquid crystals studied were synthesized by K. Fodor-Csorba. We also thank R. Pindak for several helpful conversations, and the NSF for support under grants DMR-0606160 and DMR-0964765. Use of the National Synchrotron Light Source, Brookhaven National Laboratory, was supported by the US Department of Energy, Office of Science, Office of Basic Energy Sciences, under Contract no. DE-AC02-98CH10886.

## References

1 S. H. Hong, R. Verduzco, J. C. Williams, R. J. Tweig, E. DiMasi, R. Pindak, A. Jakli, J. T. Gleeson and S. Sprunt, *Soft Matter*, 2010, **6**, 4819.
2 C. Keith, A. Lehmann, U. Baumeister, M. Prehm and C. Tschierske, *Soft Matter*, 2010, **6**, 1704.
3 N. Vaupotic, J. Szydlowska, M. Salamonczyk, A. Kovarova, J. Svoboda, M. Osipov, D. Pociecha and E. Gorecka, *Phys. Rev. E: Stat., Nonlinear, Soft Matter Phys.*, 2009, **80**, 030701.
4 O. Francescangeli, F. Vita, C. Ferrero, T. Dingemans and E. T. Samulski, *Soft Matter*, 2011, **7**, 895; O. Francescangeli and E. T. Samulski, *Soft Matter*, 2010, **6**, 2413.
5 A. de Vries, *Mol. Cryst. Liq. Cryst.*, 1970, **10**, 219; A. de Vries, *J. Phys., Colloq.*, 1975, **36**, C1.
6 B. R. Acharya, S. W. Kang, V. Prasad and S. Kumar, *J. Phys. Chem. B*, 2009, **113**, 3845.
7 J. P. Van Meter and B. H. Klanderman, *Mol. Cryst. Liq. Cryst.*, 1973, **22**, 271.
8 K. Fodor-Csorba, A. Vajda, G. Galli, A. Jakli, D. Demus, S. Holly and E. Gacs-Baitz, *Macromol. Chem. Phys.*, 2002, **203**, 1556.
9 K. C. Chu and W. L. McMillan, *Phys. Rev. A: At., Mol., Opt. Phys.*, 1977, **15**, 1181.
10 J.-H. Chen and T. C. Lubensky, *Phys. Rev. A: At., Mol., Opt. Phys.*, 1976, **14**, 1202.
11 B. S. Andereck and B. R. Patton, *J. Phys.*, 1987, **48**, 1241.
12 C. R. Safinya, R. J. Birgeneau, J. D. Litster and M. E. Neubert, *Phys. Rev. Lett.*, 1981, **47**, 668; C. R. Safinya, L. J. Martinez-Miranda, M. Kaplan, J. D. Litster and R. J. Birgeneau, *Phys. Rev. Lett.*, 1982, **50**, 56.
13 L. J. Martinez-Miranda, A. R. Kortan and R. J. Birgeneau, *Phys. Rev. Lett.*, 1986, **56**, 2264.
14 W. L. McMillan, *Phys. Rev. A: At., Mol., Opt. Phys.*, 1972, **6**, 936; W. McMillan, *Phys. Rev. A: At., Mol., Opt. Phys.*, 1973, **8**, 328.
15 M. Majumdar, P. Salamon, A. Jakli, J. T. Gleeson and S. Sprunt, *Phys. Rev. E: Stat., Nonlinear, Soft Matter Phys.*, 2011, **83**, 031701.
16 P. Sathyanarayana, M. Matthew, Q. Li, V. S. S. Sastry, B. Kundu, K. V. Le, H. Takezoe and S. Dhara, *Phys. Rev. E: Stat., Nonlinear, Soft Matter Phys.*, 2010, **81**, 010702(R).
17 J. Harden, B. Mbanga, N. Eber, K. Fodor-Csorba, S. Sprunt, J. T. Gleeson and A. Jakli, *Phys. Rev. Lett.*, 2006, **97**, 157802.
18 C. Bailey, K. Fodor-Csorba, R. Verduzco, J. T. Gleeson, S. Sprunt and A. Jakli, *Phys. Rev. Lett.*, 2009, **103**, 237803.
19 In an applied magnetic field of 1.2 T, the uniaxial order parameter of both materials is essentially unchanged from its zero field value, and there was no optical evidence of any field-induced change in the type of nematic order.
20 S. Stojadinovic, A. Adorjan, S. Sprunt, H. Sawade and A. Jakli, *Phys. Rev. E: Stat., Nonlinear, SoftMatter Phys.*, 2002, **66**, 060701.
21 A. G. Vanakaras and D. J. Photinos, *J. Chem. Phys.*, 2008, **128**, 154512.
22 B. E. Warren, *Phys. Rev.*, 1941, **59**, 693.
23 V. M. Kaganer, B. Ostrovskii and W. H. de Jeu, *Phys. Rev. A: At., Mol., Opt. Phys.*, 1991, **44**, 8158.
24 We have recently observed four lobe SAXS patterns in the nematic phase of a series of 'Y'-shaped compounds; preliminary analysis shows that these patterns are also described well by the model of eqn. (3) and (4).
25 C. Zhang, M. Gao, N. Diorio, W. Weissflog, U. Baumeister, S. Sprunt, J. T. Gleeson and A. Jakli, *Phys. Rev. Lett.*, 2012, **109**, 107802.
26 J. Seltmann, A. Marini, B. Mennucci, S. Dey, S. Kumar and M. Lehmann, *Chem. Mater.*, 2011, **23**, 2630.

 